Linearizing response of adaptive interferometer based on dynamic grating in erbium-doped fiber with saturable absorption

D. Garcia Casillas and S. Stepanov
Centro de Investigación Científica y Educación Superior de Ensenada, km. 107 carretera Tijuana-Ensenada, Ensenada, 22860, México.

M. Plata Sanchez
Instituto Nacional de Astrofísica, Óptica y Electrónica, #1 Luis Enrique Erro, Tonantzintla, Puebla, 72840, México.

Recibido el 26 de octubre de 2006; aceptado el 13 de febrero de 2007

Because of the unshifted type of recorded amplitude gratings, adaptive interferometers based on dynamic population gratings in Er-doped fibers with saturable absorption demonstrate an essentially quadratic response and, as a result, are not sensitive enough to detect a small object displacement ($\ll \lambda/4$), and cannot distinguish the displacement direction. We propose, and experimentally demonstrate, two techniques for their linearization which are based on externally introduced phase off-set between the recording interference pattern and the recorded grating. In the transient technique, the application of a fast $\pi/2$ phase jump in the detected wave makes the system response linear during the transient time of the grating formation τ_g (typically of a millisecond-submillisecond scale in Er-doped fibers). In the continuous technique, the introduction of a permanent frequency off-set $\Delta\Omega_0 \approx \tau_g^{-1}$ into the detected wave linearizes the system response permanently.

Keywords: Adaptive interferometry; population gratings; erbium-doped fiber.

La mezcla de dos ondas transitorias, empleando rejillas dinámicas de población en fibras ópticas dopadas con erbio, es atractiva para aplicaciones de detección adaptativa de vibraciones mecánicas. Dichas rejillas dinámicas pueden ser grabadas en el intervalo espectral de absorción fndamental del Er^{3+} 1480-1580 nm utilizando láseres de onda continua con potencias inferiores a 1 mW y poseen tiempos característicos de formación del orden de $\tau_g \sim$ 10-0.1 ms. Debido a la naturaleza no desplazada de las rejillas de amplitud grabadas, la configuración interferométrica muestra esencialmente una respuesta del tipo cuadrático, y como resultado, carece de sensibilidad y no es posible distinguir entre desplazamientos de direcciones opuestas de una superficie. A continuación proponemos y demostramos dos técnicas de linealización de la respuesta: del tipo transitorio, mediante la aplicación de un salto de fase auxiliar de $\pi/2$ del patrón de interferencia; y del tipo continuo, la cual utiliza un desplazamiento continuo del patrón de interferencia a la frecuencia angular óptima $\Delta\Omega_0 \approx \tau_g^{-1}$.

Descriptores: Interferometría adaptativa; rejillas de población; fibras dopadas con erbio.

PACS: 42.55.Wd; 42.65.Hw; 42.68.Wt; 42.70.Nq

Dynamic population gratings in erbium-doped fibers (EDF) are recorded by means of local saturation of the fiber optical absorption/gain in bright fringes of the interference pattern formed by two counter-propagating recording waves (see Refs. 1 to 6, and other related references in the last paper). For their recording, sub-mW light power from the spectral range 1480 – 1580 nm of the fundamental Er^{3+} absorption is usually needed. The characteristic formation/erasure time τ_g of these gratings is located in the millisecond range below the spontaneous relaxation time $\tau_0 \approx 10$ ms of the metastable state of the Er^{+3} ion.

Transient two-wave mixing (TWM) via such dynamic gratings [4-6] seems attractive for applications in the adaptive remote detection of mechanical vibrations in an industrial environment, and for detection of the laser-induced ultrasonic in particular. The diagram of the interferometric configuration, which can be used for these purposes, is presented in Fig. 1a. The dynamic grating is formed in EDF via interference of the mutually coherent direct wave R and of the back-propagating wave S, which is reflected from the vibrating object. At the photodiode, the interference of the reflected phase-modulated wave S with the diffracted from the recorded grating part of the direct wave R is detected.

For unshifted amplitude-type gratings recorded in EDF under stationary conditions, these two waves experience constructive interference and, as a result, the adaptive interferometers based on transient TWM via such gratings demonstrate a quadratic response [4-6]. In particular, in the case of rectangular phase modulation in one of the recording beams, this results in the series of the negative peaks observed in the detected output light power– see Fig. 2a. The same quadratic type of response is also observed for the unshifted gain grating recorded in optically pumped EDF, but the transient peaks are positive in this case (see Fig. 2b). Without going into detail, we can mention that, in the latter case, the experimentally observed relative TWM signal amplitude (*i.e.* that normalized to the stationary output power level) is lower; however, the transient peak relaxation is much faster.

Note that similar transient TWM via unshifted phase gratings, which are usually observed in photorefractive crystals under externally applied dc field [7], is characterized by a linear response. Here every second transient peak in the output TWM signal is of the opposite sign in the case of rectangular phase modulation. In general, because of the Kramers-Kronig relations, some admixture of the unshifted phase component is always to be present in population, *i.e.*

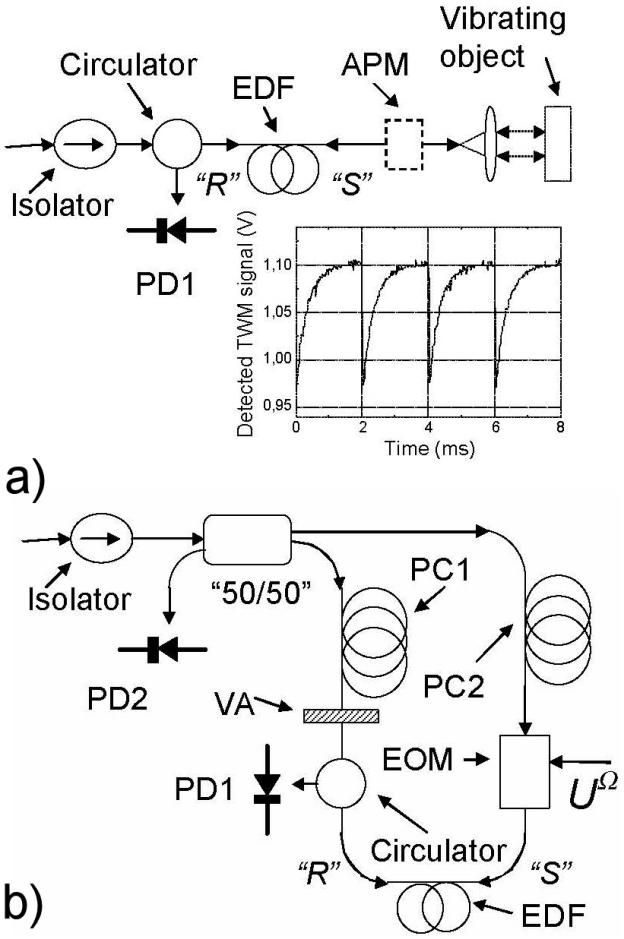

FIGURE 1. a) Diagram of linear interferometric configuration based on TWM in saturable erbium-doped fiber, which can be used for adaptive detection of mechanical vibrations. Inset presents a one-shot TWM response observed in the case of rectangular phase modulation (EDF "HG980", L = 2.9 m, λ = 1526 nm, $P_{R,in}$ = 3 mW, load resistance R = 5 kΩ, oscilloscope frequency range 20 MHz); b) diagram of the modified Sagnac interferometer used in the experiments with transient TWM in erbium-doped fiber (EOM – electro-optic modulator, PC1,2 – polarization controllers, PD1,2 – photodiodes, and VA – variable attenuator).

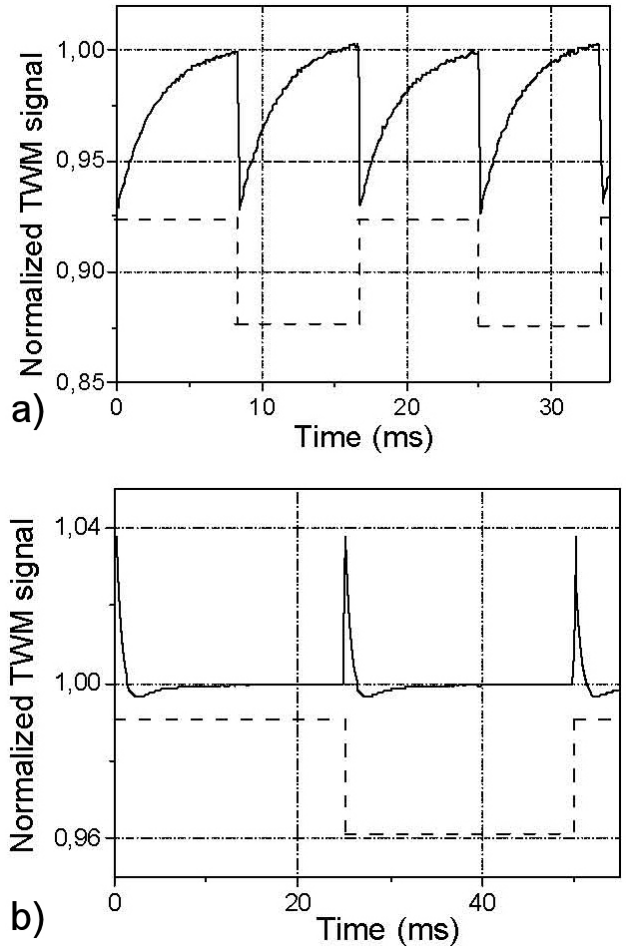

FIGURE 2. Normalized profiles of transient TWM signals observed in erbium-doped fiber without – a, and with optical pumping – b (EDF "HG980", L = 2.9 m, λ = 1549 nm, total input recording power ≈ 1 mW, pumping with two counter-propagating waves of 3.4 mW power each at λ_p = 980 nm). Dashed lines show profiles of corresponding rectangular modulation signals.

essentially amplitude, gratings recorded in EDF as well. However, the experimental data published up to now [5,6] indicate that, for the central region of Er^{+3} absorption spectrum, the phase grating contribution to the TWM signal is significantly lower than that of the amplitude grating. Our recent experiments [8] show that the phase grating is strong in the short wavelength (1480 - 1500 nm) part of this spectrum, where the fiber absorption coefficient is weaker and the sensitivity for the grating recording is significantly lower.

In this paper we concentrate on the linearization of response of the adaptive optical fiber interferometer based on unshifted amplitude gratings recorded in EDF without optical pumping. Such linearization is necessary for applications in laser vibrometers to a ensure higher detection sensitivity and a possibility of distinguishing between the opposite directions of the object displacement.

To reach this goal we propose to intentionally shifting the interferometer operation point by introducing some auxiliary phase modulation (step-like with the amplitude $\pi/2$, or sawtooth one with some resonance amplitude) into one of the recording waves. To ensure observation of linearization, we also introduce low amplitude probe sinusoidal phase modulation with a relatively high frequency $\Omega/2\pi$ = 10 kHz. Note that, in the case of the interferometer with a quadratic response, the second harmonic output signal is observed when sinusoidal phase modulation is applied [4,5]. The presence in the detected signal of a significant sinusoidal component with the fundamental modulation frequency is considered to be an indication of an effective response linearization [5,8]. In our experimental setup, both auxiliary and probe modulation signals were applied to the same phase modulator (see the oscilloscope traces of corresponding modulation signals in Figs. 3a and 4a).

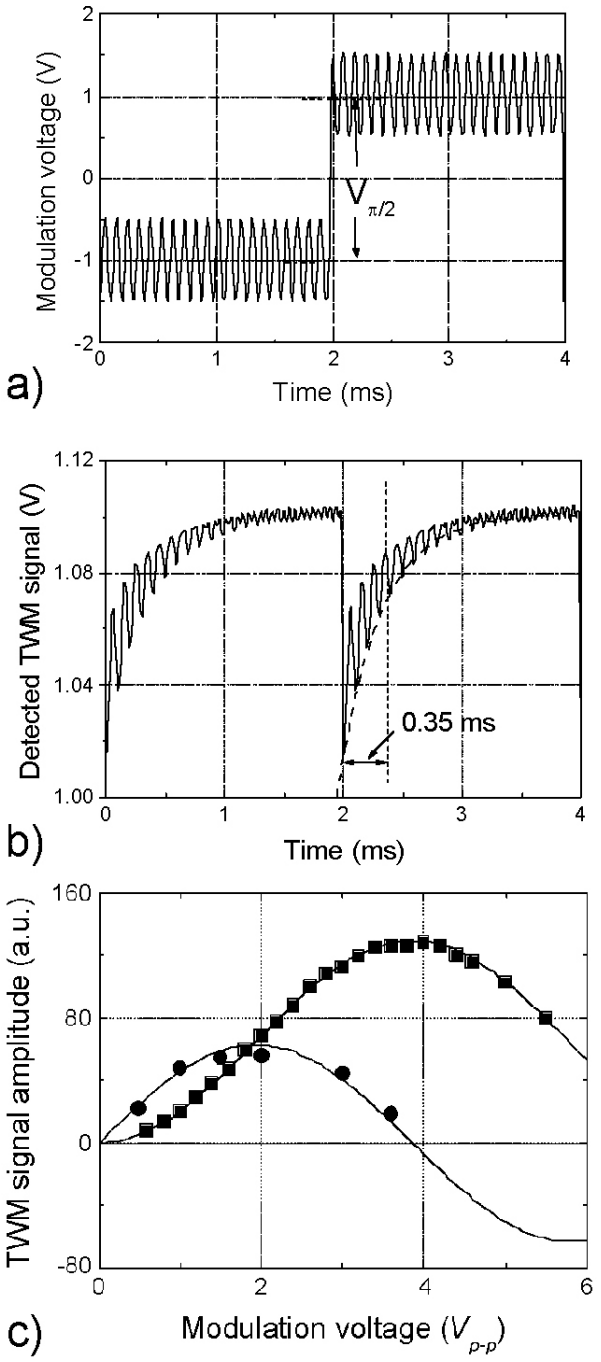

FIGURE 3. a) Modulation signal used in the experiment on observation of linearization with $\pi/2$ step-like auxiliary phase modulation, which, in addition to the rectangular component with $V_{\pi/2}$ amplitude, also includes a low-amplitude probe sinusoidal signal of 10 kHz frequency; b) Transient TWM response observed in this case, which demonstrates effective linear detection of the probe sinusoidal signal during the characteristic time of the grating formation; c) Rectangular modulation amplitude dependence of the detected probe beam amplitude (fundamental harmonic of modulation 10 kHz) - •, and that of a conventional transient TMW signal (like that presented in Fig. 2a) - (EDF "HG980", L = 2.9 m, λ = 1526 nm, $P_{R,in}$ = 3 mW, $P_{S,in}$ = 0.6 mW). Solid lines show theoretical approximation curves ($\propto \sin(\pi U/U_\pi)$ and $\propto$ [1 - $\cos(\pi U/U_\pi)$]/2 respectively, U_π = 3.8 V_{p-p}).

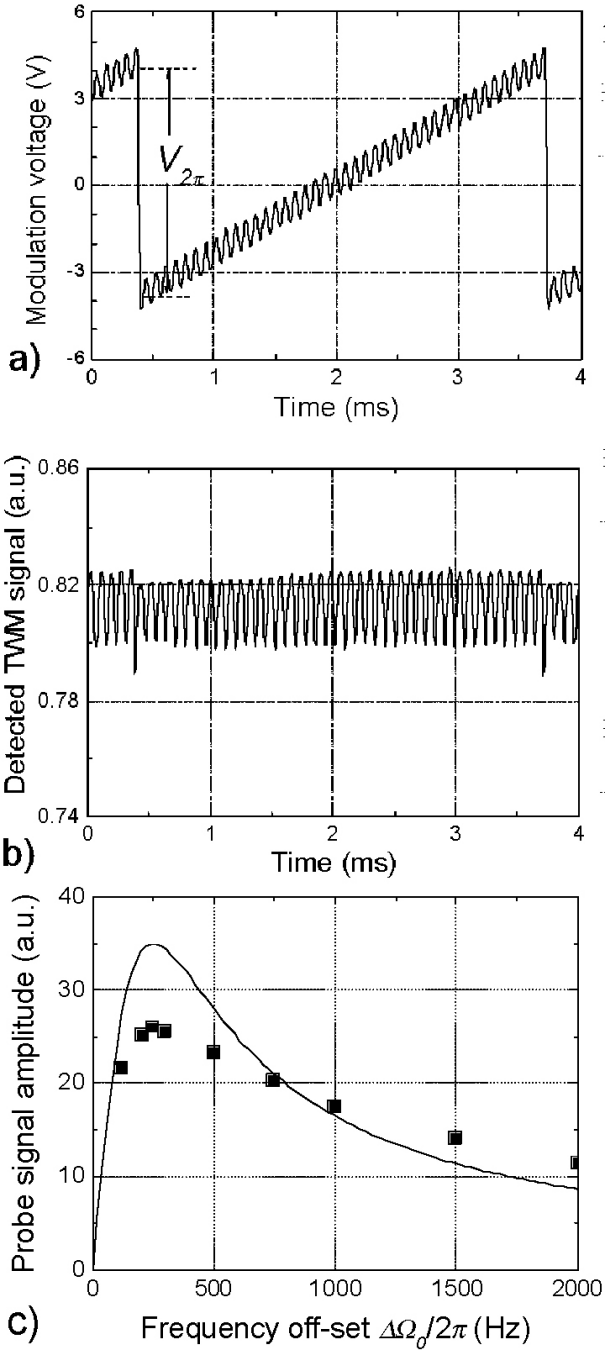

FIGURE 4. a) Modulation signal used in the experiment on observation of linearization with sawtooth auxiliary phase modulation, which, in addition to the sawtooth component with $V_{2\pi}$ amplitude, also includes low-amplitude probe sinusoidal signal of 10 kHz frequency; b) Transient TWM response observed in the case of the optimal frequency off-set, $\Delta\Omega_0/2\pi$ = 250 Hz, which demonstrates continuous linear detection of the probe sinusoidal signal; c) Amplitude of the TWM signal detected at the fundamental frequency of the probe sinusoidal modulation (10 kHz) as a function of the frequency off-set $\Delta\Omega_0$ (EDF "HG980", L = 2.9 m, λ = 1526 nm, $P_{R,in}$ = 3 mW, $P_{S,in}$ = 0.6 mW). The solid line shows the theoretical approximation by Eq.1 for τ_g = 0.64 ms.

In the experiments reported, we used a 2.9 m-long piece of OFS-Fitel "HG-980" erbium-doped fiber with initial, not saturated, absorption coefficient $\alpha_0 \approx 3$ m^{-1} and the saturation power $P_{sat} \approx 0.21$ mW at wavelength λ = 1526 nm of the distributed feedback (DFB) semiconductor laser with coherence length ≥ 20 m. No optical pumping of the fiber was used. Other experimental details, including adjustment of the recording wave polarizations and reduction of the parasitic rectangular modulation due to residual reflections from contacts between different elements of the configurations by means of averaging by digital oscilloscope, were discussed in Ref. 4 earlier. This averaging (typically over 512 shots) was also used to improve the signal-to-noise ratio in the recorded oscilloscope traces.

The experiments were performed in the configuration of the modified Sagnac interferometer presented in Fig. 1b [6,8], where two recording waves, R and S, counterpropagating through EDF, are derived from the input laser wave via a 50/50 optical coupler. Phase modulation of the wave S, which simulates the phase modulation introduced into the reflected wave by a vibrating object in the linear interferometer (Fig. 1a), is introduced via an electro-optic phase modulator (U_π = 3.8 V_{p-p}) in this configuration. The circulator, which is also introduced into the Sagnac loop interferometer, ensured observation of the output light power at one end of the fiber only. In general, the type of transient TWM response is determined by mutual phasing of the recording interference pattern and the recorded amplitude grating, and is similar for both interferometers presented in Fig. 1. Initially, both of these two interferometric configurations demonstrate the quadratic TWM response, and utilization of the proposed detection techniques linearizes response of both of them in the same way. Compared to the simpler linear arrangement, the Sagnac interferometer allowed us additional flexibility in selecting the ratio between the input powers of the recording waves, permitted the utilization of the electro-optic phase modulator with better linearity and a larger dynamic range of response, and also reduced requirements for coherence of the laser source.

In the case of rectangular auxiliary modulation (Fig. 3a), the fast displacement of the interference pattern by one-quarter of the special grating period following the $\pi/2$ phase jump, introduced into one of the recording waves, results in an instant shift of the interferometer operation point from the quadratic to the linear one. Immediately after this jump, the grating starts to adjust to a new position of the recording pattern and, for this reason, observation of the linearized response of the interferometer is possible during the grating relaxation time τ_g.

From the decay time of the detected transient TWM signal for the rectangular phase modulation, one can evaluate the grating formation time as $\tau_g \approx 0.35$ ms for the typical input powers of the recording waves $P_R \approx 3$ mW and $P_S \approx 0.6$ mW. And indeed, the sinusoidal response with a fundamental modulation frequency of 10 kHz was observed after the fast phase jump during this characteristic time only (see Fig. 3b). As one can also see from Fig. 3b, a second harmonic signal of a much smaller amplitude, which is typical for interferometer with the quadratic response, was observed after this transient period mainly. As expected, the linear sinusoidal response reached its maximum for the amplitude of auxiliary modulation $V_\pi/2$ (Fig. 3c). Figure 3c also shows that the conventional transient TWM peaks appearing in response to the rectangular phase modulation (see Fig. 2a) reach their maximum for the modulation amplitude V_π.

In the experiments with the auxiliary sawtooth signal, we used a fixed modulation amplitude equal to 2π (Fig. 4a), which resulted in a quasi-continuous movement of the recording pattern with the phase velocity $\Delta\Omega_0 = 2\pi/T$, where T is the modulation period. As was discussed earlier for similar experiments with bulk photorefractive crystals [9], the recorded dynamic grating drags behind the recording pattern in this case, and some permanent phase shift appears between them. The grating component shifted by a quarter of the spatial period, which is necessary for linear TWM response in the case under consideration, has the amplitude:

$$\delta\alpha_{\pi/2} = \delta\alpha[\Delta\Omega_0\tau_g/(1 + \Delta\Omega_0^2\tau_g^2)], \qquad (1)$$

where $\delta\alpha$ is the maximal grating amplitude recorded by the stationary pattern in EDF. This shifted grating component reaches its maximum amplitude, equal to one-half of the grating maximal stationary amplitude, at $\Delta\Omega_0\tau_g = 1$, *i.e.* when $T = 2\pi\tau_g$.

Our experiments, performed with the Er-doped fiber population gratings, confirmed the above-mentioned theoretical prediction and, indeed, an efficient and stable fundamental modulation frequency component was observed in the output signal (see Fig. 4b). The linearized TWM response efficiency reached its maximum for the off-set frequency value $\prime\Omega_0/2\pi \approx 250$ Hz under our experimental conditions, which results in the following evaluation of $\tau_g \approx 0.64$ ms. Some discrepancy with the direct evaluation of the grating relaxation time (see Fig. 3b), as well as the discrepancy between the experimentally observed off-set frequency dependence presented in Fig. 4c and the corresponding theoretical approximation by Eq. (1), can probably be attributed to the essentially non-uniform distribution of the recording light power through the fiber. As one can also see from a comparison of the oscilloscope traces presented in Figs. 3b and 4b, the sinusoidal response in the latter case proves to be lower than the maximum one observed in the case of the transient linearization immediately after the $\pi/2$ phase jump.

While our demonstration experiments were performed in the Sagnac configuration only, they are easily applicable to the linear interferometer configuration (Fig. 1a) as well. To this end, one must introduce an additional phase modulator (for example, the electro-optic one) near the output end of the linear interferometer (Fig. 1a), by which the auxiliary steplike or sawtooth phase modulation is introduced. Without discussing details, we can also mention another very important feature of this interferometric configuration. Because of

a natural imbalance between the input powers of two recording waves (the input power of the back-propagating wave S is significantly lower than that of the forward wave R), the relative amplitude of the detected TWM signal is approximately by a factor of 2 larger than in the Sagnac interferometer with equal input recording powers. As a result, even without optimization of this configuration, we could observe clear one-shot (*i.e.* obtained without averaging by digital oscilloscope) TWM signals (see inset to Fig. 1a). A detailed analysis and optimization of the linear interferometric configuration (and in particular, optimization of the EDF optical density and of the incident recording power), aimed at improving of the signal-to-noise ratio in the detected TWM signal, is in progress in our group now, and will be published later. Earlier in Ref. 6, we reported results of a similar analysis of the Sagnac interferometric configuration with equal incident powers of the recording waves.

Summarizing, we have proposed and experimentally demonstrated two techniques for linearization of adaptive interferometers based on the amplitude population gratings in erbium-doped fiber. Both of them utilize an auxiliary phase modulation introduced in one of the recording waves. In particular, it was shown that a fast phase shift by $\pi/2$ ensures transient linearization during the characteristic time of the grating formation τ_g. In its turn, the sawtooth phase modulation, which ensures optimal quasi-continuous movement of the recording interference pattern with the angular frequency $\approx \tau_g^{-1}$, results in a continuous linearization of the interferometer response. This continuity of linear operation in the latter case is paid for, however, by some reduction in the linearly detected signal amplitude.

Acknowledgements

This work was performed in partial fulfillment of CONACyT Grant 47701.

1. S. Frisken, *Opt. Lett.* **17** (1992) 1776.
2. B. Fischer, J.L. Zyskind, J.W. Sulhoff, and D.J. DiGiovanni, *Opt. Lett.* **18** (1993) 2108.
3. M.D. Feuer, *IEEE Phot. Tech. Lett.* **10** (1998) 1587.
4. S. Stepanov, E. Hernández, and M. Plata, *Opt. Lett.* **29** (2004) 1327.
5. Yu. O. Barmenkov, A.V. Kir'yanov, and M.V. Andrés, *IEEE J.Quant. Electron.* **41** (2005) 1176.
6. S. Stepanov and C. Nuñez Santiago, *Opt. Commun. 264* (2006) 105.
7. S. Stepanov, *Rep. Progress in Physics* **57** (1994) 39.
8. S. Stepanov and E. Hernández Hernández, *Opt.Commun.* **271** (2007) 91.
9. J.-P. Huignard and A. Marrakchi, *Opt.Commun.* **38** (1981) 249.